Microbiol. Immunol., **50**(4), 293–305, 2006

Immunodominant Epitope in the C-Terminus of a Variable Major Protein in *Borrelia duttonii*, an Agent of Tick-Borne Relapsing Fever

Norihiko Tabuchi*[,1], Koichiro Tomoda[1], Hiroshi Kawaguchi[1], Hiroyuki Iwamoto[2], and Masahito Fukunaga[1]

[1]*Laboratory of Molecular Microbiology, Faculty of Pharmacy and Pharmaceutical Sciences, and* [2]*Department of Applied Biological Science, Faculty of Life Science and Biotechnology, Fukuyama University, Fukuyama, Hiroshima 729–0292, Japan*

Received November 2, 2005; in revised form, January 18, 2006. Accepted January 22, 2006

***Abstract*: *Borrelia duttonii* strain Ly was isolated from a child with tick-borne relapsing fever in Tanzania. *B. duttonii* produces variable major proteins (Vmps), which undergo antigenic variation. We previously reported transcription of the *vmpP* gene, which is one of the Vmp genes in strain Ly, detected *in vitro* cultivation. In the current study, we purified the recombinant non-lipidated VmpP protein by affinity chromatography and produced VmpP polyclonal antibodies. Antigenicity of VmpP was examined by Western immunoblot analysis and peptide-based enzyme-linked immunosorbent assays. Antigenic epitopes were shown to comprise five regions interspersed within the VmpP primary amino acid sequence. Synthetic peptides spanning residues of three of five regions, 232–237 (LASIVD), 280–285 (AGGIAL), and 350–355 (KAADQQ), reacted strongly with the VmpP-specific antibody and these residues were identified as epitopes. In particular, the C-terminal domain (KAADQQ) of this protein was immunoreactive. Further research based on our results will promote the development of a recombinant vaccine for *B. duttonii* infection.**

***Key words*: *Borrelia duttonii*, Epitope, Infection, Variable major protein**

Tick-borne relapsing fever (TBRF) is characterized by cyclic spirochetemias with periodic fever, and occasionally with neurological symptoms (1). These repeated clinical manifestations are associated with antigenic changes of relapsing fever borreliae, which have been examined extensively in *Borrelia hermsii* (22, 29, 33). Antigenic variation of surface-exposed lipoproteins has been identified as an important immune evasion mechanism in relapsing fever borreliae (1–3). In a case of *B. hermsii* infection, periodic spirochetemia and fever occur when the spirochete alternates expression of at least 25 different lipoproteins that are called variable major proteins (Vmps) (34). *Borrelia burgdorferi*, an agent of Lyme disease, promotes extensive antigenic variation of outer surface Vmp-like sequences (Vls) to escape the host immune response (21, 45). The Vls locus is found on the 28-kb linear plasmid of *B. burgdorferi* strain B31 and shares some features with the antigenic variation system in *B. hermsii* (2). These proteins appear to play a pivotal role in the pathogenicity of borreliae.

In East Africa, TBRF is endemic and the causative agent, *Borrelia duttonii*, is transmitted by ticks of the genus *Ornithodoros*. Cutler et al. (9) have successfully cultivated *B. duttonii* strains in artificial BSKII medium from pediatric patients in Mvumi Hospital, Dodoma, Tanzania. The strain Ly, one of five such clinical isolates, contains a linear, 1-megabase chromosome and 12 linear plasmids of 11 to 200 kilobases in size (41). The size change of linear plasmid from 44 to 69-kb during *in vitro* cultivation of this strain caused loss of infectivity in experimental mice, leading us to believe that genes on this plasmid may be involved with infectivity in mammals. Therefore, we determined the entire nucleotide sequence of the plasmid, which had 21 *vmp* gene sequences (designated as *vmpA* to *U*) (40). To date, the complete genomic sequence of the Lyme disease spirochete *B. burgdorferi* strain B31 has revealed over 150

**Address correspondence to* Dr. Norihiko Tabuchi, Laboratory of Molecular Microbiology, Faculty of Pharmacy and Pharmaceutical Sciences, Fukuyama University, Gakuencho 1, Fukuyama, Hiroshima 729–0292, Japan. Fax: +81–849–36–2024. E-mail: tabuchi@fupharm.fukuyama-u.ac.jp

Abbreviations: bp, base pair(s); BSKII, Barbour Stoenner Kelly II; DDBJ, DNA Data Bank of Japan; GST, glutathione-*S*-transferase; PCR, polymerase chain reaction.

putative lipoprotein genes on its chromosome and plasmids (7, 15). These lipoprotein genes include outer membrane proteins associated with antigenicity (4, 10, 26), bacterial adhesion (5), and colonization in vector ticks (30, 31). Outer surface protein (Osp) A of *B. burgdorferi* was used as protective vaccine for Lyme borreliosis in the U.S. from 1999 to 2002 (39), and new vaccine candidates are considered for targeting one or more Osps and newly identified antigens such as decorin-binding protein (DbpA) and fibronectin-binding protein (BBK32) (5). In contrast, no effective vaccine for relapsing fever currently exists due in part to the lack of finding common antigens among the agents, and also due to the temporal expression of surface Vmps on the bacterial surface while in the mammalian bloodstream.

Clinical and epidemiological studies have shown that TBRF causes significant morbidity in patients under 5 years old, perinatal mortality, and morbidity (42). Therefore, TBRF vaccine would be important to control infection of spirochetes. Our previous study demonstrated that *B. duttonii* strain Ly transcribes the *vmpP* gene during early infection in gerbils and also in culture media (unpublished data). To better understand the antigenicity of VmpP and to gain insights for possible vaccine development for relapsing fever borreliae, we determined the immunodominant epitopes on VmpP of *B. duttonii* strain Ly. In this study, five epitopes were identified with specific VmpP antibodies and one on the C-terminus was recognized strongly. The C-terminal domain may thus provide a target for the development of a vaccine against *B. duttonii* infection and our results may provide the basis for the design of a vaccine based on the Vmps.

Materials and Methods

Bacterial strains and growth media. *B. duttonii* strain Ly was isolated from a 2-year-old girl with TBRF in Tanzania (9) and used for all experimental work in this study. It has been passed in broth medium continuously at least 5 times, and stored at −80 C. *B. duttonii* strain Ly was grown in Barbour-Stoenner-Kelly's (BSK) II medium supplemented with 6% rabbit serum at 32 C as described previously (40).

Recombinant plasmid construction. Three different plasmids encoding N-terminal truncated VmpP and GST fusion protein were created by PCR using *Ex Taq* polymerase (TaKaRa Bio, Kyoto, Japan). The PCR was performed with each set of the following primers: forward primers, VmpP-C15: 5′- TCC GGA TCC TGT AAT AGT GGG GGA GTA AAG-3′, VmpP-S34: 5′-

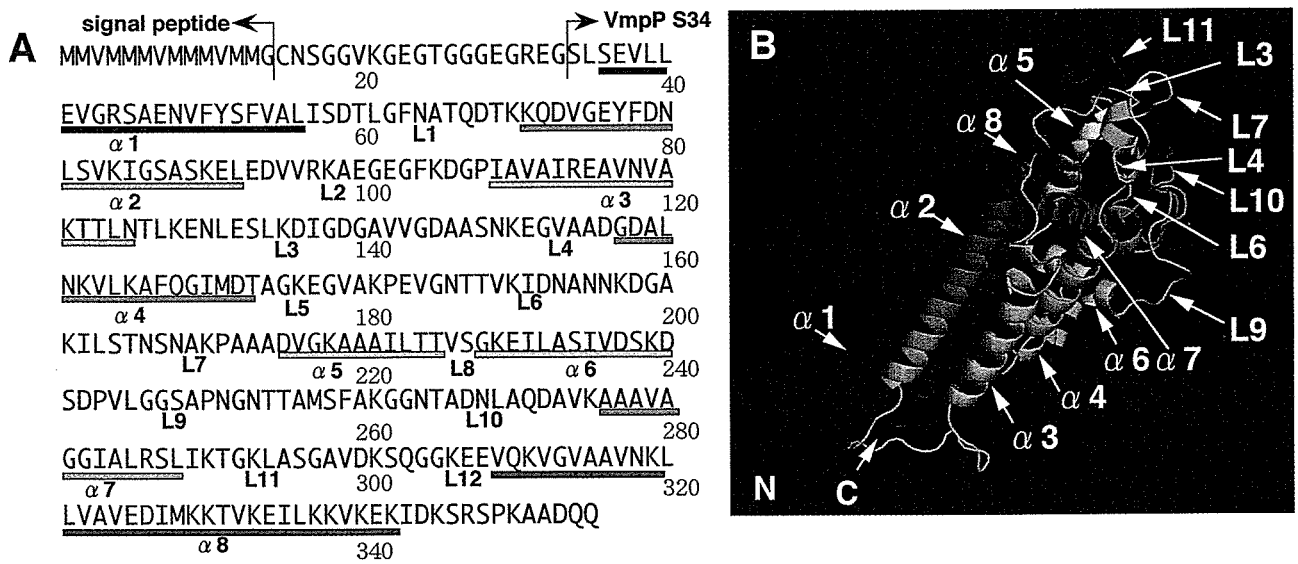

Fig. 1. Primary amino acid sequence and putative 3-D structure of VmpP. A: The primary amino acid sequence of VmpP is cited from DDBJ/EMBL/GenBank database (accession no. AB073701) (40). Amino acid number is indicated below the sequence, and putative signal sequence and VmpP-S34 regions are also shown. Presumed α-helices (α1 to α8) and short α-helices are indicated in blue characters, and loop regions (L1 to L12) in red. Color underlines for each α-helix (α1 to α8) correspond to those in the 3-D structure. B: Putative three-dimensional structure (from Gly 33 to Asp 344) of VmpP was constructed by using Swiss-Model server (http://swissmodel.expasy.org) based on the 3-D structure of *B. burgdorferi* OspC (11), and was depicted with Swiss Pdb Viewer (18). The N and C indicate the N-terminus and C-terminus of the amino acid sequence, respectively.

TCC GGA TCC AGT TTG AGT GAG GTA TTG CTG-3′, or VmpP-S58: 5′-TCC GGA TCC TCA GAT ACT TTG GGC TTT AAT-3′, reverse primer, VmpP-Rev: 5′-ATA GAG CTC *TTA* TTG CTG ATC CGC TGC CTT -3′. N-terminal amino acids of VmpP-C15, VmpP-S34, and VmpP-S58 indicate amino acid positions: Cys (position 15), Ser (position 34), and Ser (position 58), from putative initial methionine, respectively (Fig. 1A). *Bam*HI and *Sac*I recognition sequences were introduced into the forward and reverse primers, respectively (underlined sequences indicate restriction enzyme cleavage sites, and the stop codon in the reverse primer is italicized). DNA amplification using a Perkin-Elmer GeneAmp PCR System 9700 (Applied Biosystems Japan, Osaka, Japan) was performed in a thermal cycler with 25 cycles of denaturation (94 C, 30 sec), annealing (58 C, 30 sec), and extension (72 C, 1 min). The PCR product was cleaved and cloned into *Bam*HI and *Sac*I sites of pGEX-KG vector (17), and then *Escherichia coli* DH5α was transformed with the recombinant plasmid that contained the partial *vmpP* gene (pGEX-VmpP-C15 [nt 43–1070], pGEX-VmpP-S34 [nt 99–1070], and pGEX-VmpP-S58 [nt 172–1070]). Each recombinant plasmid sequence was confirmed with an automated DNA sequencer (ABI 3100 genetic analyzer; Applied Biosystems) by using a Big dye terminator cycle sequencing kit (Applied Biosystems).

Expression and purification of GST-VmpP fusion protein. Recombinant plasmids were purified from *E. coli* DH5α cells and then transformed into *E. coli* BL21 (DE3) cells. Transformants were grown overnight at 37 C in 2× YT medium (tryptone 8 g, yeast extracts 5 g, and NaCl 2.5 g in 500 ml) containing ampicillin (100 μg/ml). Fifty milliliters of the overnight culture was transferred into 500 ml of 2× YT broth and incubated for 3 hr at 37 C. Induction of the fusion proteins was performed by addition of 0.1 mM isopropyl-β-D-thiogalactopyranoside (IPTG) and incubation was continued for 3 hr at 25 C. The three fusion proteins were expressed and each protein was purified as described below. In brief, *E. coli* cells were collected by centrifugation and the fusion protein was released by sonication. Cell debris was removed by centrifugation, and supernatant was then applied to a Glutathione-Sepharose 4B column (Amersham Pharmacia Biotech, Uppsala, Sweden). After washing the column with PBS, the fusion proteins were digested with thrombin, and the truncated VmpP protein (aa 34–355) was eluted from the column. The purity and molecular size of the protein was verified by SDS-PAGE, and the N-terminal amino acid sequence of the protein was confirmed by using PPSQ-10 protein sequencer (Shimadzu, Tokyo).

Development of rabbit Anti-VmpP polyclonal antibody. Two Japanese White rabbits (2.0 kg) were used for development of antibodies. Primary immunizations were done with subcutaneous footpad injections of 400 μg of purified VmpP-S34 protein in Freund's complete adjuvant (1:1 in volume, Difco Laboratories, Detroit, Mich., U.S.A.). After 14 days, each animal received an intradermal boost with 200 μg of VmpP-S34 protein in Freund's incomplete adjuvant (1:1 in volume). Intradermal injection in the dorsal skin was done every 2 weeks until a clear arthus reaction became visible. Each rabbit was bled from the ear vein 7 days after the last injection. Blood was centrifuged and the serum was collected. Immunoglobulin G was purified from the serum by using an MAb Trap kit (Amersham Pharmacia Biotech) according to the manufacturer's recommendation. Antibody purities were examined by SDS-PAGE and antibodies were stored at −20 C.

Construction of plasmids containing vmpP *gene fragments.* Based on the *vmpP* gene sequence, the primers shown in Tables 1 and 2 were synthesized and used to amplify gene fragments encoding partial VmpP peptides. The reverse primer was designed with a stop codon upstream of the *Sac*I cleavage site. DNA amplifications were performed in a thermal cycler with 25 cycles of denaturation (94 C, 30 sec), annealing (58 C, 30 sec), and extension (72 C, 10 sec). Each DNA fragment was digested with *Bam*HI and *Sac*I enzymes and ligated into the pGEX-KG vector at the same restriction enzyme sites. The recombinant plasmid was introduced into *E. coli* DH5α cells and propagated. Plasmid DNA was then extracted, purified, and sequenced, and was then used to transform *E. coli* BL21(DE3) cells. Procedures for cultivation of bacterial cells, IPTG induction, and purification of the fusion protein were the same as described above.

SDS-PAGE and Western blotting. Cultured cell lysates (10 μg each) were subjected to SDS-PAGE according to Laemmli's method (25) using 12.5% acrylamide under reduced conditions. The gel was processed for Western blot analysis with antibody against VmpP according to standard procedures (43). The samples were boiled for 5 min with buffer (125 mM Tris-HCl, 3% SDS, 5% β-mercaptoethanol, 10% glycerol, 0.01% bromophenol blue, pH 6.8) and resolved by gel electrophoresis. The gel was stained with Coomassie brilliant blue R-250, and proteins were transferred to a nitrocellulose membrane (Bio-Rad Laboratories, Hercules, Calif., U.S.A.) for 2 hr at 2 mA/cm^2 by ElectroBlotter (ATTO, Osaka, Japan) using a transfer buffer (25 mM Tris, 200 mM glycine, 5% methanol). The membrane was blocked by incubation in TBST (20 mM Tris-HCl, 0.15 M NaCl, and 0.1% Tween 20, pH

Table 1. Primers for 30 amino acid fragments of VmpP employed in this study

Primer	Sequence (5′ to 3′)[a]	Fragment
BdVmpP C15	TCCGGATCCTGTAATAGTGGGGGAGTAAAG	f1
BdVmpP R1	ATAGAGCTC*TTA*TCTCCCTACTTCCAGCAA	
BdVmpP F2	TCCGGATCCCTGGAAGTAGGGAGAAGTGCA	f2
BdVmpP R2	ATAGAGCTC*TTA*TGTATCTTGAGTTGCATT	
BdVmpP F3	TCCGGATCCGCAACTCAAGATACAAAGAAG	f3
BdVmpP R3	ATAGAGCTC*TTA*ATCTTCTAACTCTTTTGA	
BdVmpP F4	TCCGGATCCAAAGAGTTAGAAGATGTAGTA	f4
BdVmpP R4	ATAGAGCTC*TTA*AACATTAACTGCTTCTCT	
BdVmpP F5	TCCGGATCCGAAGCAGTTAATGTTGCCAAG	f5
BdVmpP R5	ATAGAGCTC*TTA*ACCTACCACAGCTCCATC	
BdVmpP F6	TCCGGATCCGGAGCTGTGGTAGGTGATGCA	f6
BdVmpP R6	ATAGAGCTC*TTA*TCCTTGAAATGCTTTAAG	
BdVmpP F7	TCCGGATCCAAAGCATTTCAAGGAATAATG	f7
BdVmpP R7	ATAGAGCTC*TTA*TGCATTATCTATTTTTAC	
BdVmpP F8	TCCGGATCCAAAATAGATAATGCAAATAAT	f8
BdVmpP R8	ATAGAGCTC*TTA*TGCCTTTCCTACATCTGC	
BdVmpP F9	TCCGGATCCGATGTAGGAAAGGCAGCAGCT	f9
BdVmpP R9	ATAGAGCTC*TTA*TACAGGATCACTATCTTT	
BdVmpP F10	TCCGGATCCGATAGTGATCCTGTACTAGGA	f10
BdVmpP R10	ATAGAGCTC*TTA*TAAATTATCTGCAGTATT	
BdVmpP F11	TCCGGATCCACTGCAGATAATTTAGCACAA	f11
BdVmpP R11	ATAGAGCTC*TTA*TAATTTTCCTGTCTTAAT	
BdVmpP F12	TCCGGATCCAAGACAGGAAAATTAGCATCA	f12
BdVmpP R12	ATAGAGCTC*TTA*CTTATTTACTGCGGCTAC	
BdVmpP F13	TCCGGATCCGCCGCAGTAAATAAGCTATTA	f13
BdVmpP Rev	ATAGAGCTC*TTA*TTGCTGATCCGCTGCCTT	

[a] Underlines indicate the restriction enzyme sites (*Bam*HI and *Sac*I) and italics indicate stop codons.

8.0) with 10% skim milk, and was then incubated with anti-VmpP-S34 antibody (1:500 dilution) or anti-GST Tag™ monoclonal antibody (1:1,000 dilution) (Novagen, Darmstadt, Germany). Secondary antibodies were sheep anti-mouse IgG and donkey anti-rabbit IgG coupled to horseradish peroxidase (Amersham), and were used at a concentration of 1:10,000 dilution. The immunoreacting bands were detected using an enhanced chemiluminescence (ECL) detection kit (Amersham) or chemiluminescent peroxidase substrate (Sigma-Aldrich, St. Louis, Mo., U.S.A.). The protein concentration was determined using a Bradford protein assay kit (Bio-Rad Laboratories) and bovine serum albumin (BSA) was used as a standard. Densitometric analyses of protein bands were performed on a scanned digital gel image with an Interigent Quantifier (Bio Image, Relyon, Tokyo).

Synthetic peptides. Peptides spanning the entire immunoreactive regions (f3-b, f6-c, f9-b, f11-c, and f13-d fragments; each peptide consisted of 15 amino acids) of VmpP were synthesized as 8-mers or 7-mers overlapping each other by 4 amino acid residues. Lyophilized peptides (Sigma-Aldrich Corporation) were maintained as a concentrated stock (2–5 mg/ml) in 100% DMSO and diluted in the appropriate solution prior to immediate use.

Peptide-based enzyme-linked immunosorbent assay (ELISA). Each well of Maxsorp, 96-well ELISA plates (Nalge-Nunc, Roskilde, Denmark) was coated for 1 hr at 37 C by adding 100 µl of binding buffer (1 M sodium carbonate, pH 9.6) containing 10 µM of each peptide. The plate was washed four times with 300 µl of PBS supplemented with 1.0% BSA and was subsequently blocked by incubation with PBS-Tween (PBS-T) supplemented with 1.0% (wt/vol) BSA fraction V (Sigma) for 2 hr at room temperature. Polyclonal anti-VmpP rabbit IgG (diluted with 0.5% BSA containing 1 µg/ml PBS-T) was added to the wells, and the plate was then incubated for 2 hr at 37 C. Wells were washed four times with PBS-T and bound antibodies were detected by using *p*-nitrophenyl phosphate (1 mg/ml of diethanolamine buffer, pH 9.6) as a substrate and 10,000-fold diluted alkaline phosphatase-conjugated anti-rabbit total IgG (Sigma). The mixture was allowed to develop for 20 min and the reaction was stopped by addition of 50 µl of 0.5 N NaOH. The optical density at 405 nm (OD_{405}) was measured with a plate reader, ImmunoMini NJ-2300 (Nalge-Nunc). Results are

Table 2. Primers for 15 amino acid fragments of VmpP employed in this study

Primer	Sequence (5′ to 3′)[a]	Fragment
BdVmpP F3-1	TCCGGATCCGCAACTCAAGATACAAAGAAG	f3-a
BdVmpP R3-1	ATAGAGCTC*TTA*GTCAAAATATTCTCCTAC	
BdVmpP F3-2	TCCGGATCCGATGTAGGAGAATATTTTGAC	f3-b
BdVmpP R3-2	ATAGAGCTC*TTA*CGATCCAATCTTAACACT	
BdVmpP F3-3	TCCGGATCCAATTTAAGTGTTAAGATTGGA	f3-c
BdVmpP R3-3	ATAGAGCTC*TTA*ATCTTCTAACTCTTTTGA	
BdVmpP F6-1	TCCGGATCCGGAGCTGTGGTAGGTGATGCA	f6-a
BdVmpP R6-1	ATAGAGCTC*TTA*CGCTACTCCTTCTTTATT	
BdVmpP F6-2	TCCGGATCCAGTAATAAAGAAGGAGTAGCG	f6-b
BdVmpP R6-2	ATAGAGCTC*TTA*TTTATTTAATGCATCACC	
BdVmpP F6-3	TCCGGATCCGCAGATGGTGATGCATTAAAT	f6-c
BdVmpP R6-3	ATAGAGCTC*TTA*TCCTTGAAATGCTTTAAG	
BdVmpP F9-1	TCCGGATCCGATGTAGGAAAGGCAGCAGCT	f9-a
BdVmpP R9-1	ATAGAGCTC*TTA*TTTACCACTTACTGTTGT	
BdVmpP F9-2	TCCGGATCCCTAACAACAGTAAGTGGTAAA	f9-b
BdVmpP R9-2	ATAGAGCTC*TTA*GTCAACTATTGATGCTAA	
BdVmpP F9-3	TCCGGATCCGAAATATTAGCATCAATAGTT	f9-c
BdVmpP R9-3	ATAGAGCTC*TTA*TACAGGATCACTATCTTT	
BdVmpP F11-1	TCCGGATCCACTGCAGATAATTTAGCACAA	f11-a
BdVmpP R11-1	ATAGAGCTC*TTA*TACTGCCGCTGCTTTAAC	
BdVmpP F11-2	TCCGGATCCGCAGTTAAAGCAGCGGCAGTA	f11-b
BdVmpP R11-2	ATAGAGCTC*TTA*TGAACGTAGGGCTATTCC	
BdVmpP F11-3	TCCGGATCCGCAGGAGGAATAGCCCTACGT	f11-c
BdVmpP R11-3	ATAGAGCTC*TTA*TAATTTTCCTGTCTTAAT	
BdVmpP F13-1	TCCGGATCCGCCGCAGTAAATAAGCTATTA	f13-a
BdVmpP R13-1	ATAGAGCTC*TTA*TTTCATTATATCTTCTAC	
BdVmpP F13-2	TCCGGATCCGTAGAAGATATAATGAAAAAA	f13-b
BdVmpP R13-2	ATAGAGCTC*TTA*TTTTTTAAGTATTTCTTT	
BdVmpP F13-3	TCCGGATCCAAAGAAATACTTAAAAAAGTA	f13-c
BdVmpP R13-3	ATAGAGCTC*TTA*CCTTGATTTATCTATTTT	
BdVmpP F13-4	TCCGGATCCAAAATAGATAAATCAAGGTCT	f13-d
BdVmpP Rev	ATAGAGCTC*TTA*TTGCTGATCCGCTGCCTT	

[a] Underlines indicate the restriction enzyme sites (*Bam*HI and *Sac*I) and italics indicate stop codons.

expressed as means±standard deviations and the mean values of six independent experiments were calculated for each analysis. Statistical differences in OD_{405} values were assessed by one-factor ANOVA, followed by a post hoc test (Bonferroni/Dunn test). Statistical significance was defined as $P<0.05$ and $P<0.01$.

Nucleotide sequence accession numbers. The VmpP, VmpG, VmpL, and VmpK sequences of the *B. duttonii* strain Ly have been assigned DDBJ/EMBL/GenBank accession number AB073701 (40). The accession numbers of *B. hermsii* Vmp sequences published previously (6, 34) are as follows: Vmp7, X53926; Vmp18, U52149; Vmp21, M57256; Vmp25, L04787.

Results

Putative VmpP Structure

The structural model of VmpP was obtained by homology modeling based on *B. burgdorferi* OspC X-ray structure (PDB ID 1G5Z) (11) using Swiss-Model server (http://swissmodel.expasy.org) (18, 32, 38) (Fig. 1). Putative VmpP structure was similar to the OspC structure of *B. burgdorferi*, whereas the amino acid similarity was low (17.2%). VmpP is composed of 355 amino acids including the signal peptide, and the molecular weight of the mature protein was 34,766 (Fig. 1A). The putative 3-D structure of a single molecule has eight long α-helices (α1 to α8), five short α-helices (fewer than 7 amino acids each), and twelve connecting loop regions (L1 to L12). As shown in Fig. 1B, the eight α-helices are α1 (aa 36–56), α2 (aa 71–92), α3 (aa 109–125), α4 (aa 157–173), α5 (aa 215–225), α6 (aa 228–240), α7 (aa 276–288), and α8 (aa 309–342), and connecting loops.

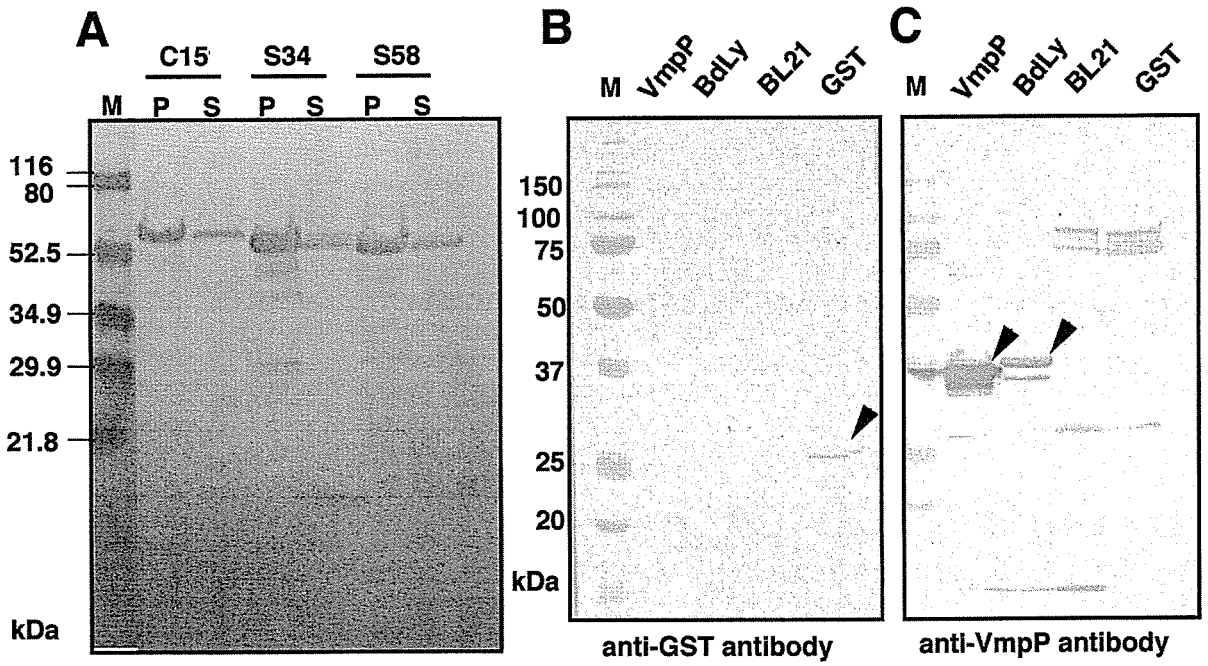

Fig. 2. Expression of GST-recombinant VmpP proteins and development of a specific polyclonal antibody for VmpP. A: Expression of serial N-terminal-truncated VmpP (GST-VmpP-C15, GST-VmpP-S34, GST-VmpP-S58) was analyzed by immunoblotting. After induction of fusion protein with IPTG, *E. coli* BL21 cells were sonicated, and the supernatant separated (S) from cell debris (precipitation, P) by centrifugation. Equal amounts (10 μg) of both fractions were applied on SDS-PAGE followed by Western blotting with monoclonal anti-GST antibody (1:1,000). Lanes: M, prestained SDS-PAGE standards low range marker (Bio-Rad Laboratories); P, precipitation; S, supernatant. GST-VmpP-S34 fusion protein was purified from supernatant (S34, lane S) and VmpP-S34 was eluted from the Glutathione-Sepharose 4B column with thrombin digestion. The antibody raised against VmpP-S34 was developed in rabbits. B and C: Purified VmpP-S34 protein, cells of *B. duttonii* strain Ly, *E. coli* BL21 cell lysate, and induced GST protein in *E. coli* BL21 were applied on SDS-PAGE and examined by Western immunoblotting analysis (B: anti-GST antibody, 1:1,000, C: anti-VmpP-S34 antibody 1:500). Lanes: M, precision plus protein™ dual color standards marker (Bio-Rad Laboratories); VmpP, purified VmpP-S34 (1 μg); BdLy, 10 μg protein of cultured *B. duttonii* strain Ly whole cell; BL21, *E. coli* BL21 without pGEX-KG vector (10 μg protein); GST, *E. coli* BL21 with pGEX-KG vector after induction of IPTG (10 μg protein). Arrowhead in Fig. B indicates GST (26-kDa) protein. Arrowheads shown in Fig. C indicate the purified VmpP-S34 (lane VmpP) and native VmpP (lane BdLy), respectively.

VmpP Fusion Protein

Western blot analysis using anti-GST antibody is shown in Fig. 2A. The molecular mass of each protein was 61-kDa (GST-VmpP-C15), 59-kDa (GST-VmpP-S34), and 57-kDa (GST-VmpP-S58). These mobilities corresponded to putative molecular weights. Most of the fusion protein was recovered in insoluble fraction (Fig. 2A, lanes P) and a part of the expressed protein was released to the soluble fraction. Fusion protein in soluble fraction was collected and purified by means of a GST-Sepharose column. Western blots using anti-GST antibody or anti-VmpP antibody are shown in Fig. 2B and 2C. As seen in Fig. 2C, anti-VmpP antibody reacted strongly with purified VmpP-S34 protein (lane VmpP) and the native VmpP protein band in whole cell lysate of *B. duttonii* strain Ly (lane BdLy). The molecular weight of VmpP-S34 was 33.2-kDa with a purity of over 95%, and the final yield was 5 mg per liter of culture (data not shown). The N-terminal amino acid sequence of this purified protein was SLSEVLLE, which was identical to the deduced sequence.

Reactivity of Anti-Recombinant VmpP Polyclonal Antibody with VmpP Fragments

Thirteen adjacent overlapping regions of VmpP were produced as GST fusion proteins. Each fusion protein has 30 amino acids of VmpP except the last (f13), which included 40 amino acids. The 33 amino acid amino-terminus that included the signal peptide was excluded from the analysis (Fig. 3A). All GST-fusion proteins were separated on SDS-PAGE gels, and examined with Western blot analysis. All proteins (f2 to f13) were recognized by a monoclonal antibody to GST, as indicated by the presence of bands at expected molecu-

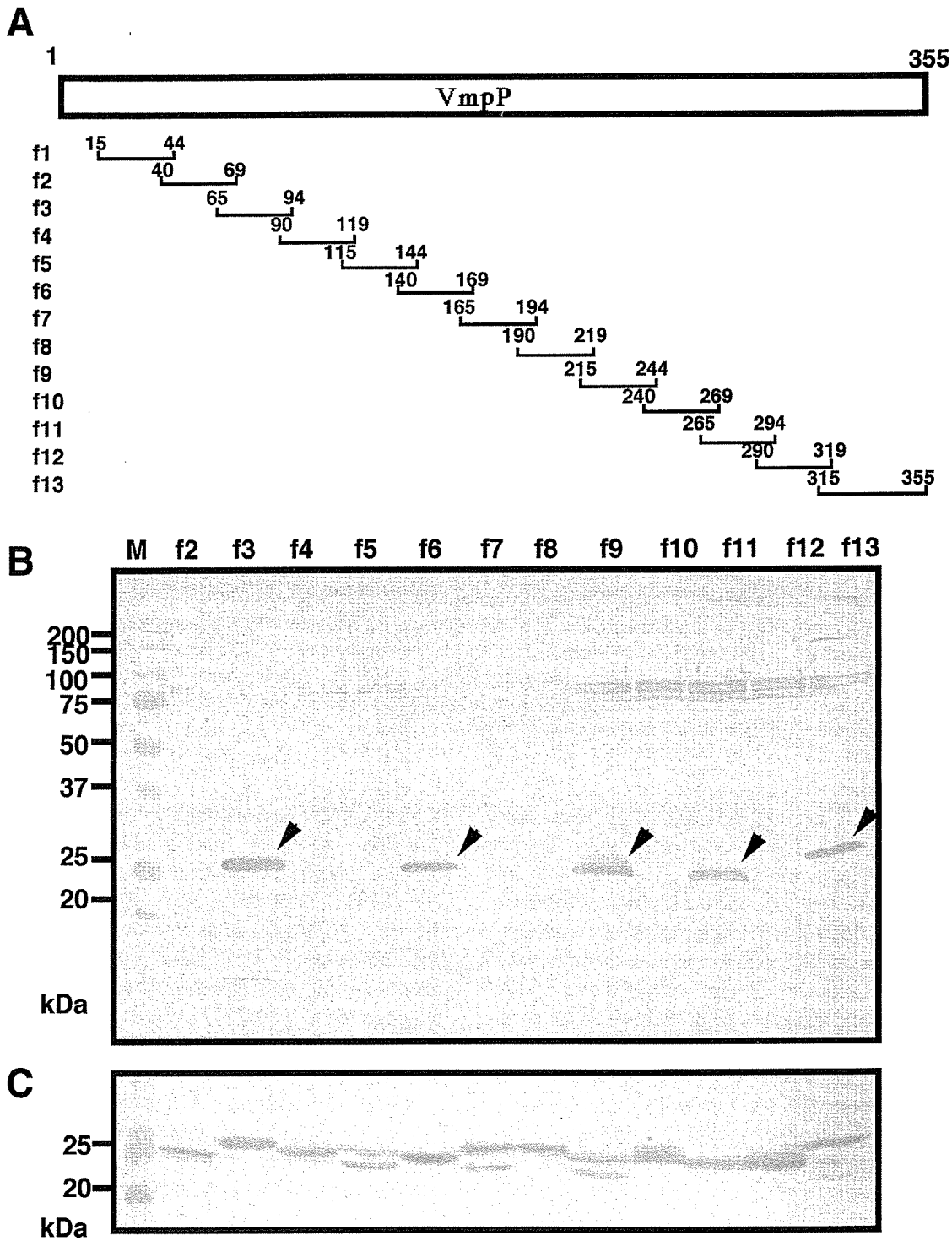

Fig. 3. Identification of antigenic regions of VmpP by immunoblot analysis. A: A schematic representation of the VmpP protein (355 amino acids) is shown. Each nucleotide fragment encoding 30 amino acids (f1 to f12; f13 has 41 aa) is designated and synthesized by PCR as described in "Materials and Methods." All fragments are designated to overlap 5 amino acid residues with each other. B: Each fragment was inserted into the vector and the GST fusion protein was expressed in *E. coli* BL21 cells. Fusion proteins were separated by SDS-PAGE, transferred onto nitrocellulose membranes, and incubated with rabbit anti-VmpP antibody (1:500). Arrowheads (lanes f3, f6, f9, f11, and f13) indicate the anti-VmpP antibody-reacting peptides. Lanes: M, precision plus protein™ dual color standards marker (Bio-Rad Laboratories); f2 to f13, whole-cell lysate of *E. coli* BL21 cells expressing each fragment. C: Fusion proteins were also analyzed by Western blotting with mouse monoclonal anti-GST antibody (1:1,000). Lanes are the same as in Fig. 4B.

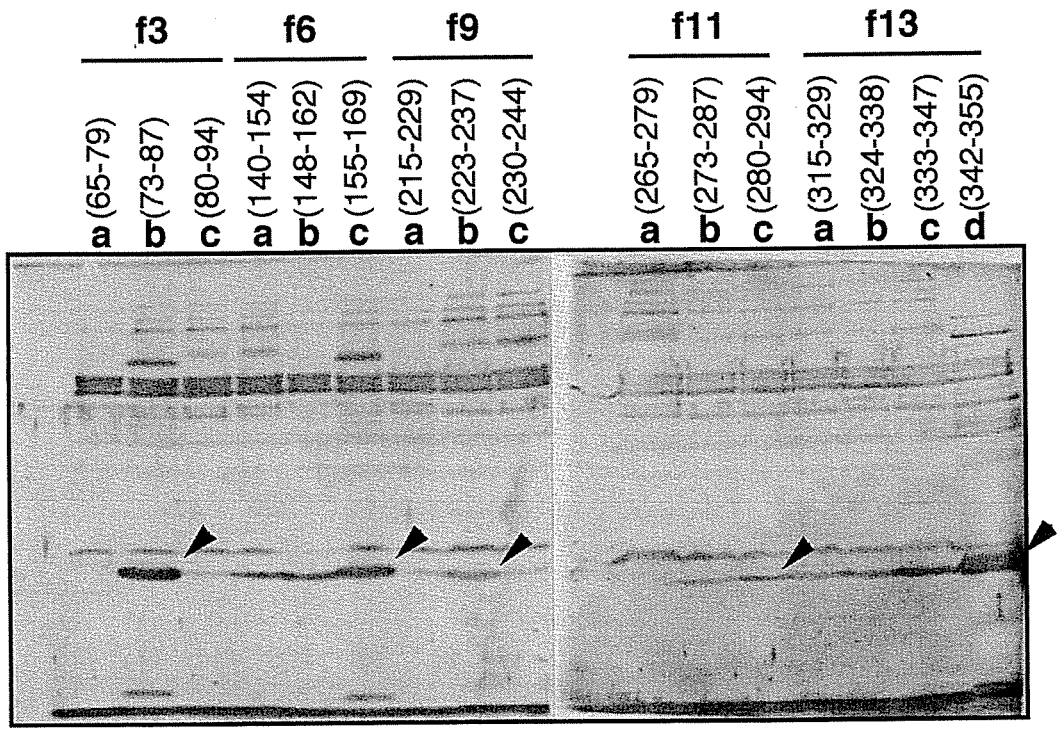

Fig. 4. Western blot analysis of epitope regions of VmpP with specific antibody. The fragments (f3, f6, f9, f11, and f13) are divided into 3 or 4 fragments encoding 15 amino acids overlapping seven to eight amino acids (f13 fragments overlapped six amino acid residues each) and were expressed in *E. coli* BL21. Fusion proteins were separated by SDS-PAGE, transferred onto nitrocellulose membranes, and incubated with rabbit anti-VmpP antibody (1:500). Arrowheads indicate the immunodominant regions (f3-b, f6-c, f9-b, f11-c, and f13-d).

lar masses (Fig. 3C). However, anti-VmpP-S34 antibodies reacted with five VmpP fragments, f3 (aa 65–94), f6 (aa 140–169), f9 (aa 215–244), f11 (aa 265–294), and f13 (aa 315–355) (Fig. 3B). Moreover, we constructed three DNA fragments (four fragments for f13) encoding 15 amino acid residues encompassing each antibody-reacting fragment. GST fusion proteins were produced and analyzed with Western blotting as explained previously. VmpP antibody reacted intensively with f3-b (aa 73–87), f6-c (aa 155–169), f9-b (aa 223–237), f11-c (aa 280–294), and f13-d (aa 342–355) (Fig. 4). Weak signals were detected on f6-b and f13-c, indicating that the epitope of f6 and f13 extended over these two fragments.

Identification of Immunodominant Epitopes of VmpP Using Peptide-Based ELISA

The epitopes recognized by anti-VmpP-S34 antibody were composed of five main regions (f3-b, f6-c, f9-b, f11-c, and f13-d). In order to define the core of the epitope, 15 peptides encompassing the five anti-VmpP antibody-reacting fragments were synthesized, and their reactivities examined with anti-VmpP antibody. Quantitative peptide-based ELISA data are shown in Fig. 5. Statistical significance was achieved in the peptides f9-b, f11-c, and f13-d. Significant differences ($P<0.05$) between f9-bM (0.254 ± 0.069) and f9-bR (0.398 ± 0.107), and between f11-cL (0.424 ± 0.117) and f11-cM (0.272 ± 0.088), were observed. At $P<0.01$, f13-dR (0.523 ± 0.132) demonstrated significant absorbance compared to f13-dM (0.323 ± 0.017). These results indicate that antigenic VmpP epitopes consist of hexapeptides: LASIVD (f9-bR, aa 232 to 237), AGGIAL (f11-cL, aa 280 to 285), and KAADQQ (f13-dR, aa 350 to 355).

The deduced amino acid sequences of Vmps from *B. duttonii* strain Ly and *B. hermsii* were aligned and identified five epitopes (Fig. 6). The overall amino acid sequence similarities ranged from 43.7 to 74.4% except the VmpL by using DNASTAR (DNASTAR, Inc., Madison, Wis., U.S.A.). Epitopes (hexapeptides) in the f3-bR, f6-cL, and f13-dR were located on variable regions, while those of f9-bR and f11-cL were on relatively conserved regions. The C-terminus region (f13-dR, KAADQQ) of VmpP was variable and predominantly epitope.

Discussion

In this study, we analyzed the reactivities of poly-

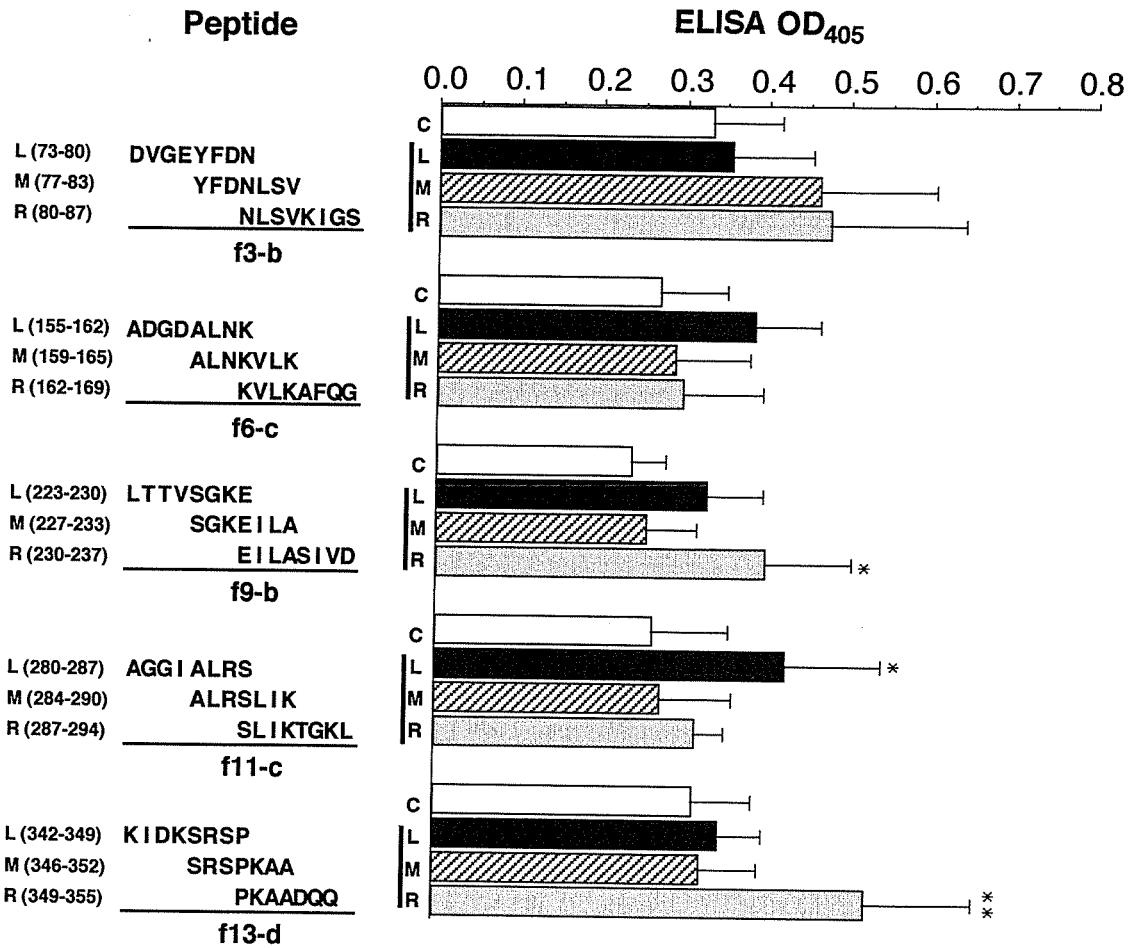

Fig. 5. Synthetic peptides reacted with anti-VmpP antibody as analyzed by ELISA. Synthesized peptides are 8-mers or 7-mers overlapping each other by 4 amino acids. Using these peptides covering five epitope regions, quantitative peptide-based ELISA was performed with anti-VmpP polyclonal antibody (1:500). The OD_{405} values of the six independent experiments were analyzed by one-factor ANOVA, followed by a post hoc test (Bonferroni/Dunn test). Control bar (C) at each peptide group indicates the six independent values by using pre-immune rabbit serum (1:500). Each value represents the mean±S.D. Statistical significance was defined as $*P<0.05$ and $**P<0.01$.

clonal VmpP antibodies and epitopes of the protein. We identified five epitopes that were comprised of at least six amino acid residues. Antigenic epitopes on VmpP were scattered throughout the primary sequence. In particular, the C-terminus region was strongly reactive with polyclonal VmpP antibody and may have an immunodominant epitope. These antigenic epitopes of VmpP were assessed with the Hopp-Wood hydrophilicity algorithm (19). The VmpP fragment which contained the antigenic determinant for the specific antibody was located in a highly hydrophilic region of VmpP and was thus suitable as an epitope for B-cells (19). The average hydrophilicity values for the hexapeptides within the C-terminal amino acid residues (positions 340 to 355) ranged from 0.967 to 1.967. The C-terminal region of VmpP would therefore be conformationally flexible and extruded from the surface of the spirochete.

B. burgdorferi produces abundant amounts of OspA and OspB in unfed ticks, and rapidly down-regulates these proteins during feeding. In contrast, OspC expression is up-regulated during mammalian infection (37). Recently, Mathiesen et al. (27, 28) reported that the OspC of the Lyme disease spirochete *Borrelia garinii* had one single major immunodominant epitope of the C-terminal amino acid sequence PVVAESPKKP which is accessible to antibodies in Lyme disease patients. The C-terminus of native OspC was flexible and extruded from the outer surface of the spirochetes (24). Moreover, by using epitope mapping, Sears et al. (35) reported that the C-terminal of *B. burgdorferi* OspA become an important protective epitope. This region is structurally distinct from the rest of the OspA. The three-dimensional structure shows that OspA of *B.*

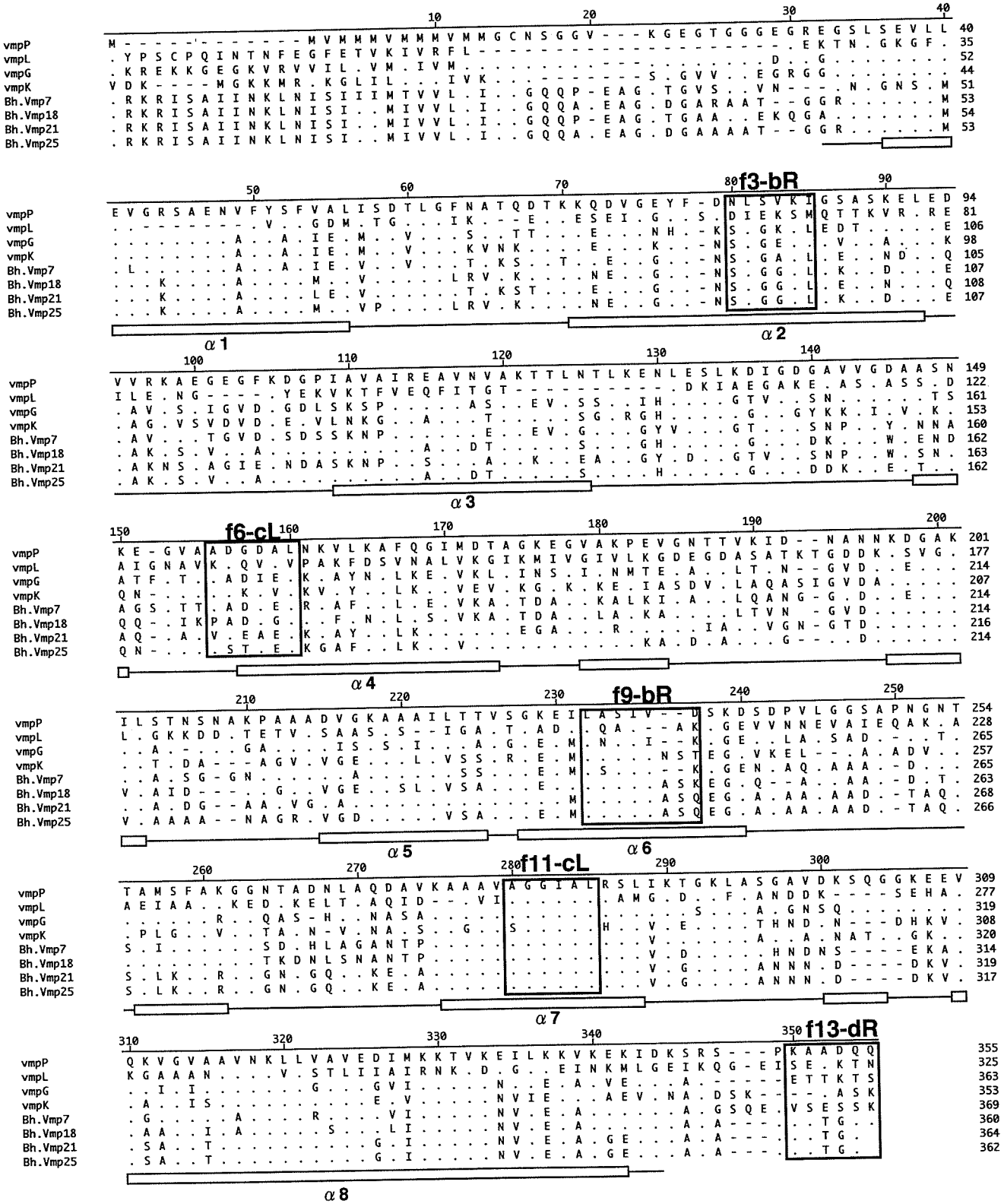

Fig. 6. Comparison of Vmp amino acid sequences for *B. duttonii* and *B. hermsii*. The sequences used in this comparison were as follows: deduced amino acid sequence of the vmpP, vmpL, vmpG, and vmpK of *B. duttonii* strain Ly (40) and *B. hermsii* HS1 (Bh.) vmp7, vmp18, vmp21, and vmp25 (6, 34). Boxes indicate epitope regions. Dots represent identical amino acids and dashes correspond to deleted amino acids. Putative secondary structure of VmpP is indicated under the sequence alignments. The amino acid sequence alignments were performed with the DNASTAR program (DNASTAR, Inc.).

burgdorferi strain B31 is folded into 21 consecutive anti-parallel β-strands connected by turns or short loops, followed by a single surface-exposed C-terminal α-helix (26). The C-terminus of OspA is also recognized by two murine monoclonal antibodies LA-2 and C3.78, which have complement-independent bactericidal activity (20, 26). Furthermore, the bactericidal antigen binding fragments (Fabs) H6831 and monoclonal antibody CB2 recognize the C-terminal fragment of *B. burgdorferi* OspB (4, 8, 12). Thus, the C-termini of the lipoproteins of Lyme disease borreliae Osps may stimulate targeting antibodies in the hosts (13, 14, 16, 36). It is considered that the C-termini of the Vmp protein family of relapsing fever borreliae may be predominant B-cell epitopes for antibodies on these regions. Therefore, VmpP might also have a C-terminal immunodominant epitope that induces bactericidal activity.

Prophylactic vaccines are currently being developed (44), one of which is already commercially available (39). The OspA C-terminal fragment has been incorporated into a second-generation vaccine by Koide et al. (23). Moreover, a recent study indicates the OspA function of the *B. burgdorferi* which colonizes the tick midgut via tick receptor for OspA (TROSPA), the *Ixodes scapularis* tick midgut receptor; this receptor is also being considered for a new vaccine target (31). The development of a relapsing fever vaccine is hampered by antigenical complexities of these spirochetes. Mice immunized with recombinant VmpP in our preliminary experiments were only partially protected when challenged with spirochetes (data not shown). These reasons for incomplete protection are being considered now.

The three-dimensional structure of VmpP is currently unknown, but evidence does implicate it as an important virulence factor in the mammalian host. The sequence conservation of the f9-bR and f11-cL regions across Vmps within the organism and *B. hermsii* vmps indicates that these regions are important in some aspect of the physiology of *B. duttonii* (Fig. 6). Therefore, one would not expect these sequences to be antigenic in hosts during a relapsing fever borrelia infection. These regions may be inaccessible to antibodies, either because of their conformation or subsurface location. Moreover, antigenicity of epitopes was supported by the predicted structure of VmpP (Figs. 1 and 6). Our results showed that the four immunogenic regions of f3-bR, f6-cL, f9-bR and f11-cL, but not f13-dR, are included on a part of the α-helices (α2, α4, α6, and α7), but not the distal loop regions from the borrelial outer membrane. Therefore, the C-terminus (f13-dR) of VmpP might become a predominant epitope.

In this study, we identified the antigenic epitopes of VmpP at the molecular level. The immunogenic regions are confined to a small portion of the protein. Common antigenic determinants from VmpP of *B. duttonii* may be useful in the production of a synthetic vaccine and in the determination of three-dimensional structures of VmpP and other Vmp proteins of spirochetemias. To develop a recombinant vaccine for *B. duttonii* infection, we need further experiments about the reactivity for VmpP to anti-sera of other experimental animals and relapsing fever patients with *B. duttonii* infection in Tanzania.

We would like to thank Tom Schwan and Ellen Carlin for their comments, which have greatly improved this manuscript. We also thank Masaya Ohta and Fumito Matsuura for providing the peptide sequencing technique and apparatus. This study was supported in part by Grants-in-Aid for Scientific Research from the Ministry of Education, Culture, Sports, Science and Technology, Japan to N.T. (number 17790294), by Health Science Grants for Research on Emerging and Re-emerging Infectious Diseases from the Ministry of Health, Labour and Welfare, Japan, and by Green Science Research Center, Fukuyama University.

References

1) Barbour, A.G. 1990. Antigenic variation of a relapsing fever *Borrelia* species. Annu. Rev. Microbiol. **44**: 155–171.
2) Barbour, A.G., and Restrepo, B.I. 2000. Antigenic variation in vector-borne pathogens. Emerg. Infect. Dis. **6**: 449–457.
3) Barstad, P.A., Coligan, J.E., Raum, M.G., and Barbour, A.G. 1985. Variable major proteins of *Borrelia hermsii*. Epitope mapping and partial sequence analysis of CNBr peptides. J. Exp. Med. **161**: 1302–1314.
4) Becker, M., Bunikis, J., Lade, B.D., Dunn, J.J., Barbour, A.G., and Lawson, C.L. 2005. Structural investigation of *Borrelia burgdorferi* OspB, a bactericidal Fab target. J. Biol. Chem. **280**: 17363–17370.
5) Brown, E.L., Kim, J.H., Reisenbichler, E.S., and Höök, M. 2005. Multicomponent Lyme vaccine: three is not a crowd. Vaccine **23**: 3687–3696.
6) Burman, N., Bergström, S., Restrepo, B.I., and Barbour, A.G. 1990. The variable antigens Vmp7 and Vmp21 of the relapsing fever bacterium *Borrelia hermsii* are structurally analogous to the VSG proteins of the African trypanosome. Mol. Microbiol. **4**: 1715–1726.
7) Casjens, S., Palmer, N., van Vugt, R., Huang, W.M., Stevenson, B., Rosa, P., Lathigra, R., Sutton, G., Peterson, J., Dodson, R.J., Haft, D., Hickey, E., Gwinn, M., White, O., and Fraser, C.M. 2000. A bacterial genome in flux: the twelve linear and nine circular extrachromosomal DNAs in an infectious isolate of the Lyme disease spirochete *Borrelia burgdorferi*. Mol. Microbiol. **35**: 490–516.
8) Coleman, J.L., Rogers, R.C., Rosa, P.A., and Benach, J.L. 1994. Variations in the ospB gene of *Borrelia burgdorferi* result in differences in monoclonal antibody reactivity and in production of escape variants. Infect. Immun. **62**: 303–307.

9) Cutler, S.J., Akintunde, C.O., Moss, J., Fukunaga, M., Kurtenbach, K., Talbert, A., Zhang, H., Wright, D.J., and Warrell, D.A. 1999. Successful *in vitro* cultivation of *Borrelia duttonii* and its comparison with *Borrelia recurrentis*. Int. J. Syst. Bacteriol. **49**: 1793–1799.
10) Eicken, C., Sharma, V., Klabunde, T., Lawrenz, M.B., Hardham, J.M., Norris, S.J., and Sacchettini, J.C. 2002. Crystal structure of Lyme disease variable surface antigen VlsE of *Borrelia burgdorferi*. J. Biol. Chem. **277**: 21691–21696.
11) Eicken, C., Sharma, V., Klabunde, T., Owens, R.T., Pikas, D.S., Höök, M., and Sacchettini, J.C. 2001. Crystal structure of Lyme disease antigen outer surface protein C from *Borrelia burgdorferi*. J. Biol. Chem. **276**: 10010–10015.
12) Escudero, R., Halluska, M.L., Backenson, P.B., Coleman, J.L., and Benach, J.L. 1997. Characterization of the physiological requirements for the bactericidal effects of a monoclonal antibody to OspB of *Borrelia burgdorferi* by confocal microscopy. Infect. Immun. **65**: 1908–1915.
13) Fikrig, E., Tao, H., Barthold, S.W., and Flavell, R.A. 1995. Selection of variant *Borrelia burgdorferi* isolates from mice immunized with outer surface protein A or B. Infect. Immun. **63**: 1658–1662.
14) Fikrig, E., Tao, H., Kantor, F.S., Barthold, S.W., and Flavell, R.A. 1993. Evasion of protective immunity by *Borrelia burgdorferi* by truncation of outer surface protein B. Proc. Natl. Acad. Sci. U.S.A. **90**: 4092–4096.
15) Fraser, C.M., Casjens, S., Huang, W.M., Sutton, G.G., Clayton, R., Lathigra, R., White, O., Ketchum, K.A., Dodson, R., Hickey, E.K., Gwinn, M., Dougherty, B., Tomb, J.F., Fleischmann, R.D., Richardson, D., Peterson, J., Kerlavage, A.R., Quackenbush, J., Salzberg, S., Hanson, M., van Vugt, R., Palmer, N., Adams, M.D., Gocayne, J., Weidman, J., Utterback, T., Watthey, L., McDonald, L., Artiach, P., Bowman, C., Garland, S., Fujii, C., Cotton, M.D., Horst, K., Roberts, K., Hatch, B., Smith, H.O., and Venter, J.C. 1997. Genomic sequence of a Lyme disease spirochaete, *Borrelia burgdorferi*. Nature **390**: 580–586.
16) Golde, W.T., Piesman, J., Dolan, M.C., Kramer, M., Hauser, P., Lobet, Y., Capiau, C., Desmons, P., Voet, P., Dearwester, D., and Frantz, J.C. 1997. Reactivity with a specific epitope of outer surface protein A predicts protection from infection with the Lyme disease spirochete, *Borrelia burgdorferi*. Infect. Immun. **65**: 882–889.
17) Guan, K.L., and Dixon, J.E. 1991. Eukaryotic proteins expressed in *Escherichia coli*: an improved thrombin cleavage and purification procedure of fusion proteins with glutathione *S*-transferase. Anal. Biochem. **192**: 262–267.
18) Guex, N., and Peitsch, M.C. 1997. SWISS-MODEL and the Swiss-PdbViewer: an environment for comparative protein modeling. Electrophoresis **18**: 2714–2723.
19) Hopp, T.P., and Woods, K.R. 1981. Prediction of protein antigenic determinants from amino acid sequences. Proc. Natl. Acad. Sci. U.S.A. **78**: 3824–3828.
20) Johnson, B.J., Sviat, S.L., Happ, C.M., Dunn, J.J., Frantz, J.C., Mayer, L.W., and Piesman, J. 1995. Incomplete protection of hamsters vaccinated with unlipidated OspA from *Borrelia burgdorferi* infection is associated with low levels of antibody to an epitope defined by mAb LA-2. Vaccine **13**: 1086–1094.
21) Kawabata, H., Myouga, F., Inagaki, Y., Murai, N., and Watanabe, H. 1998. Genetic and immunological analyses of Vls (VMP-like sequences) of *Borrelia burgdorferi*. Microb. Pathog. **24**: 155–166.
22) Kitten, T., and Barbour, A.G. 1990. Juxtaposition of expressed variable antigen genes with a conserved telomere in the bacterium *Borrelia hermsii*. Proc. Natl. Acad. Sci. U.S.A. **87**: 6077–6081.
23) Koide, S., Yang, X., Huang, X., Dunn, J.J., and Luft, B.J. 2005. Structure-based design of a second-generation Lyme disease vaccine based on a C-terminal fragment of *Borrelia burgdorferi* OspA. J. Mol. Biol. **350**: 290–299.
24) Kumaran, D., Eswaramoorthy, S., Luft, B.J., Koide, S., Dunn, J.J., Lawson, C.L., and Swaminathan, S. 2001. Crystal structure of outer surface protein C (OspC) from the Lyme disease spirochete, *Borrelia burgdorferi*. EMBO J. **20**: 971–978.
25) Laemmli, U.K. 1970. Cleavage of structural proteins during the assembly of the head of bacteriophage T4. Nature **227**: 680–685.
26) Li, H., Dunn, J.J., Luft, B.J., and Lawson, C.L. 1997. Crystal structure of Lyme disease antigen outer surface protein A complexed with an Fab. Proc. Natl. Acad. Sci. U.S.A. **94**: 3584–3589.
27) Mathiesen, M.J., Christiansen, M., Hansen, K., Holm, A., Åsbrink, E., and Theisen, M. 1998. Peptide-based OspC enzyme-linked immunosorbent assay for serodiagnosis of Lyme borreliosis. J. Clin. Microbiol. **36**: 3474–3479.
28) Mathiesen, M.J., Holm, A., Christiansen, M., Blom, J., Hansen, K., Østergaard, S., and Theisen, M. 1998. The dominant epitope of *Borrelia garinii* outer surface protein C recognized by sera from patients with neuroborreliosis has a surface-exposed conserved structural motif. Infect. Immun. **66**: 4073–4079.
29) Meier, J.T., Simon, M.I., and Barbour, A.G. 1985. Antigenic variation is associated with DNA rearrangements in a relapsing fever *Borrelia*. Cell **41**: 403–409.
30) Pal, U., de Silva, A.M., Montgomery, R.R., Fish, D., Anguita, J., Anderson, J. F., Lobet, Y., and Fikrig, E. 2000. Attachment of *Borrelia burgdorferi* within *Ixodes scapularis* mediated by outer surface protein A. J. Clin. Investig. **106**: 561–569.
31) Pal, U., Li, X., Wang, T., Montgomery, R.R., Ramamoorthi, N., Desilva, A.M., Bao, F., Yang, X., Pypaert, M., Pradhan, D., Kantor, F.S., Telford, S., Anderson, J.F., and Fikrig, E. 2004. TROSPA, an *Ixodes scapularis* receptor for *Borrelia burgdorferi*. Cell **119**: 457–468.
32) Peitsch, M.C. 1995. Protein modelling by E-mail. Bio/Technology **13**: 658–660.
33) Plasterk, R.H., Simon, M.I., and Barbour, A.G. 1985. Transposition of structural genes to an expression sequence on a linear plasmid causes antigenic variation in the bacterium *Borrelia hermsii*. Nature **318**: 257–263.
34) Restrepo, B.I., Kitten, T., Carter, C.J., Infante, D., and Barbour, A.G. 1992. Subtelomeric expression regions of *Borrelia hermsii* linear plasmids are highly polymorphic. Mol. Microbiol. **6**: 3299–3311.
35) Sears, J.E., Fikrig, E., Nakagawa, T.Y., Deponte, K., Mar-

cantonio, N., Kantor, F.S., and Flavell, R.A. 1991. Molecular mapping of Osp-A mediated immunity against *Borrelia burgdorferi*, the agent of Lyme disease. J. Immunol. **147**: 1995–2000.

36) Schubach, W.H., Mudri, S., Dattwyler, R.J., and Luft, B.J. 1991. Mapping antibody-binding domains of the major outer surface membrane protein (OspA) of *Borrelia burgdorferi*. Infect. Immun. **59**: 1911–1915.

37) Schwan, T.G. 2003. Temporal regulation of outer surface proteins of the Lyme-disease spirochaete *Borrelia burgdorferi*. Biochem. Soc. Trans. **31**: 108–112.

38) Schwede, T., Kopp, J., Guex, N., and Peitsch, M.C. 2003. SWISS-MODEL: an automated protein homology-modeling server. Nucleic Acids Res. **31**: 3381–3385.

39) Steere, A.C., Sikand, V.K., Meurice, F., Parenti, D.L., Fikrig, E., Schoen, R.T., Nowakowski, J., Schmid, C.H., Laukamp, S., Buscarino, C., Krause, D.S., and the Lyme Disease Vaccine Study Group. 1998. Vaccination against Lyme disease with recombinant *Borrelia burgdorferi* outer-surface lipoprotein A with adjuvant. N. Engl. J. Med. **339**: 209–215.

40) Tabuchi, N., Mitani, H., Seino, S., and Fukunaga, M. 2002. The 44-kb linear plasmid molecule in the relapsing fever agent *Borrelia duttonii* strain Ly serve as a preservation of *vmp* genes. Microbiol. Immunol. **46**: 159–165.

41) Takahashi, Y., Cutler, S.J., and Fukunaga, M. 2000. Size conversion of a linear plasmid in the relapsing fever agent *Borrelia duttonii*. Microbiol. Immunol. **44**: 1071–1074.

42) Talbert, A., Nyange, A., and Molteni, F. 1998. Spraying tick-infested houses with lambda-cyhalothrin reduces the incidence of tick-borne relapsing fever in children under five years old. Trans. R. Soc. Trop. Med. Hyg. **92**: 251–253.

43) Towbin, H., Staehelin, T., and Gordon, J. 1979. Electrophoretic transfer of proteins from polyacrylamide gels to nitrocellulose sheets: procedure and some applications. Proc. Natl. Acad. Sci. U.S.A. **76**: 4350–4354.

44) Wallich, R., Jahraus, O., Stehle, T., Tran, T.T., Brenner, C., Hofmann, H., Gern, L., and Simon, M.M. 2003. Artificial-infection protocols allow immunodetection of novel *Borrelia burgdorferi* antigens suitable as vaccine candidates against Lyme disease. Eur. J. Immunol. **33**: 708–719.

45) Zhang, J.R., Hardham, J.M., Barbour, A.G., and Norris, S.J. 1997. Antigenic variation in Lyme disease borreliae by promiscuous recombination of VMP-like sequence cassettes. Cell **89**: 275–285.

J Mol Evol (2006) 63:251–261
DOI: 10.1007/s00239-005-0196-y

JOURNAL OF MOLECULAR EVOLUTION

Molecular Mechanisms for the Variation of Mitochondrial Gene Content and Gene Arrangement Among Chigger Mites of the Genus *Leptotrombidium* (Acari: Acariformes)

Renfu Shao,[1,2] Stephen C. Barker,[2] Harumi Mitani,[1] Mamoru Takahashi,[3] Masahito Fukunaga[1]

[1] Faculty of Pharmacy and Pharmaceutical Sciences, Fukuyama University, Fukuyama, Hiroshima 729-0292, Japan
[2] School of Molecular and Microbial Sciences, The University of Queensland, Brisbane, Queensland 4072, Australia
[3] Kawagoe Sogo Senior High School, Kawagoe, Saitama 350-0036, Japan

Received: 12 August 2005 / Accepted: 18 April 2006 [*Reviewing Editor:* Dr. Martin Kreitman]

Abstract. The gene content of a mitochondrial (mt) genome, i.e., 37 genes and a large noncoding region (*LNR*), is usually conserved in Metazoa. The arrangement of these genes and the *LNR* is generally conserved at low taxonomic levels but varies substantially at high levels. We report here a variation in mt gene content and gene arrangement among chigger mites of the genus *Leptotrombidium*. We found previously that the mt genome of *Leptotrombidium pallidum* has an extra gene for large-subunit rRNA (*rrnL*), a pseudo-gene for small-subunit rRNA (*PrrnS*), and three extra *LNR*s, additional to the 37 genes and an *LNR* typical of Metazoa. Further, the arrangement of mt genes of *L. pallidum* differs drastically from that of the hypothetical ancestor of the arthropods. To find to what extent the novel gene content and gene arrangement occurred in *Leptotrombidium*, we sequenced the entire or partial mt genomes of three other species, *L. akamushi*, *L. deliense*, and *L. fletcheri*. These three species share the arrangement of all genes with *L. pallidum*, except *trnQ* (for tRNA-glutamine). Unlike *L. pallidum*, however, these three species do not have extra *rrnL* or *PrrnS* and have only one extra *LNR*. By comparison between *Leptotrombidium* species and the ancestor of the arthropods, we propose that (1) the type of mt genome present in *L. pallidum* evolved from the type present in the other three *Leptotrombidium* species, and (2) three molecular mechanisms were involved in the evolution of mt gene content and gene arrangement in *Leptotrombidium* species.

Key words: Concerted evolution — Genome evolution — Gene order — Gene rearrangement — *Leptotrombidium* — Mitochondrial genome — mtDNA recombination

Introduction

Evolutionary biologists have been increasingly using data from entire mitochondrial (mt) genomes, including nucleotide sequence and gene arrangement, to study the evolutionary history of Metazoa (e.g., von Nickisch-Rosenegk et al. 2001; Grande et al. 2002; Ingman and Gyllensten 2003; Scouras et al. 2004; Macaulay et al. 2005). To date, mt genomes of over 620 species of Metazoa have been sequenced (see http://evogen.jgi.doe.gov/top_level/organelles.html). The vast majority of these genomes are circular, are about 15 kb long, and have 37 genes and a single large noncoding region (*LNR*). These 37 genes encode the large- and small-subunit rRNAs of the mt ribosome, 13 proteins for oxidative phosphorylation, and 22 tRNAs for the translation of the proteins encoded by mt genomes (Boore 1999). So the gene content of the mt genome is highly conserved in

Correspondence to: Renfu Shao; *email:* r.shao@uq.edu.au

Metazoa. The arrangement of genes in the mt genome of Metazoa is generally conserved at low taxonomic levels, such as within a genus or family, but varies substantially at high levels, such as among phyla (Boore 1999). Indeed, there are more than 120 types of gene arrangement among the species of Metazoa that have been sequenced for entire mt genomes (counted from the web site above). The difference between any two types of gene arrangement can be in the position and/or the orientation of transcription of one or more genes or blocks of genes. A gene or a block of genes may change its position and/or the orientation of transcription in an mt genome by (1) translocation to a near site in the genome, (2) translocation to a distant site in the genome, (3) inversion and translocation, (4) inversion but not translocation, and (5) gene shuffling, where most genes in a genome are translocated and/or inverted.

Comparison of the arrangement of mt genes has been shown to be a powerful tool for phylogenetic studies (Boore and Brown 1998; Dowton et al. 2002). Yet we still do not know much about how the various arrangements of mt genes evolved in Metazoa. To date, four molecular mechanisms have been proposed to account for rearrangement of mt genes in Metazoa: (1) tandem duplication of a section of a genome followed by *random* deletion of excess genes (Moritz and Brown 1986; Boore 2000), (2) tandem duplication followed by *transcription-orientation-dependent* deletion of excess genes (Lavrov et al. 2002), (3) nonhomologous *intra*genome recombination (Lunt and Hyman 1997; Dowton and Campbell 2001), and (4) nonhomologous *inter*genome recombination (Boore 2000; Shao et al. 2005a). Among these four mechanisms, tandem duplication followed by random deletion is relatively well supported (Moritz and Brown 1986; Boore 2000); there is limited evidence so far for the other three mechanisms.

We recently reported that the mt genome of a chigger mite, *Leptotrombidium pallidum*, has a novel gene content—it has an extra gene for large-subunit rRNA, a pseudo-gene for small-subunit rRNA, and three extra *LNR*s, additional to the 37 genes and *LNR* that are typical of Metazoa (Shao et al. 2005a). Further, the arrangement of mt genes of *L. pallidum* differs drastically from that of the hypothetical ancestor of the arthropods. To find to what extent the novel gene content and gene arrangement occurred in *Leptotrombidium*, we sequenced the entire mt genomes of two more *Leptotrombidium* species, *L. akamushi* and *L. deliense*, and the partial mt genome of another species, *L. fletcheri*. We found that these three species have a type of mt genome that differs from that of *L. pallidum* in both gene content and gene arrangement. By comparison between *Leptotrombidium* species and the ancestor of the arthropods, we propose that (1) the type of mt genome present in *L. pallidum* evolved from the type present in the other three *Leptotrombidium* species, and (2) three molecular mechanisms were involved in the evolution of mt gene content and gene arrangement in *Leptotrombidium* species.

Table 1. Primers used to amplify the mitochondrial genomes of *Leptotrombidium akamushi* (La), *L. deliense* (Ld), and *L. fletcheri* (Lf)

Primer	Sequence (5′ to 3′)
La-cox1F	GATACTTATTATGTAGTCGCCCAT
La-nad6R	ATAGTTAATATTGAAATTCTAATG
La-nad6F	CTAGTATGAAATATTAGCATGCTT
La-cox1R	CCAAAGCCTGGTAGAATGAGGATG
Ld-cox1F	AGATGTAGATTCTCGAGCTTATTT
Ld-cobR	TACATCTCGTGAGATATGAATAAC
Ld-nad6F	TATCAAAATTGATGAATAGTTATT
Ld-cox1R	GTAAGTCCTCCAATTGTGAATAAA
Lf-nad1F	AGGAGAATCAGAATTAGTCTCAGGATTTAA
Lf-nad4R	ATGGCTACCAAAGGCTCATGTGGAGGCTCC
Lf-cox3F	AGCTTGATATTGACATTTTGTTGATGTAGT
Lf-nad5R	AGTTCATTCTTCTACCTTAGTGACAGCTGG

Materials and Methods

Specimen Collection, DNA Extraction, PCR Amplification, Genome Sequencing, and Annotation

L. akamushi, *L. deliense*, and *L. fletcheri* were from colonies reared in our laboratory. *L. akamushi* was originally from a Japanese grass vole, *Microtus montebelli*, from the Akiata Prefecture of Japan. *L. deliense* and *L. fletcheri* were originally from the former U.S. Army Medical Research Unit at the Institute for Medical Research in Kuala Lumpur, Malaysia. Genomic DNAs were extracted from five adult *L. akamushi* and five adult *L. deliense* using the method detailed by Shao et al. (2004) and one adult *L. fletcheri* using the DNeasy Tissue Kit (QIAGEN). The entire mt genomes of *L. akamushi* and *L. deliense* were amplified in two overlapping fragments (6.4 and 7.3 kb) by long-PCR and were then sequenced by a shotgun method. Two sections (3.1 and 1.6 kb) of the mt genome of *L. fletcheri* that were particularly pertinent to this study were amplified by PCR and were then sequenced by primer walking. PCR primers were (1) La-cox1F with La-nad6R, and La-nad6F with La-cox1R, for *L. akamushi*; (2) Ld-cox1F with Ld-cobR, and Ld-nad6F with Ld-cox1R, for *L. deliense*; and (3) Lf-nad1F with Lf-nad4R, and Lf-cox3F with Lf-nad5R, for *L. fletcheri* (Table 1). Our methods for PCR amplification, shotgun sequencing, and mt genome annotation were described by Shao et al. (2005a). The sequences of the mt genomes of *L. akamushi*, *L. deliense*, and *L. fletcheri* were deposited in DDBJ and GenBank under accession numbers AB191044-5 and AY973038-9.

Construction of Secondary Structures of Large- and Small-Subunit rRNAs

To identify the domains that are absent in the rRNAs of *Leptotrombidium* species, we constructed the secondary structures of the large- and small-subunit rRNAs of *L. pallidum*. We retrieved the secondary structure of the large-subunit rRNA of the hard tick, *Ixodes hexagonus*, from the European ribosomal RNA database (http://www.psb.ugent.be/rRNA/) and used it as a template to construct the putative secondary structure of the large-subunit

rRNA of *L. pallidum*. We chose *I. hexagonus* because it was most closely related to *L. pallidum* among the arthropods whose secondary structures of large-subunit rRNAs were available in the database. There was no secondary structure of small-subunit rRNA of chelicerates (ticks, mites, and their kin) in the database; only those of insects and crustaceans were available. So we constructed the putative secondary structure of the small-subunit rRNA of *L. pallidum* using that of the fruit fly, *Drosophila yakuba*, as a template.

Phylogenetic Analyses of Nucleotide Sequences of Large Noncoding Regions

We inferred the phylogeny of the *LNR*s of the four *Leptotrombidium* species to discover whether the *LNR*s of each species had evolved independently or in concert. Nucleotide sequences of the *LNR*s were aligned with ClustalX (Thompson et al. 1997). For both pairwise and multiple-sequence alignments, the gap-opening penalty was 15.00, the gap-extension penalty 2.00, and the DNA weight matrix IUB. For multiple-sequence alignments, the delay-divergent sequence was set at 30% and the DNA-transition-weight was 0.50. Neighbor-joining (NJ), maximum-likelihood (ML), and maximum-parsimony (MP) trees were inferred with PAUP 4.0b10 (Swofford 2000). The general time-reversible model and the gamma-distributed rates were used in ML analysis; the instantaneous rate matrix, base frequencies, and shape of the gamma distribution were estimated by PAUP. Bootstrap analyses (1000 replicates) were done with the NJ, ML, and MP trees.

Results

Variation in Mitochondrial Genome Size, Gene Content, and Gene Arrangement Among Leptotrombidium *Species*

We sequenced the entire mt genomes of *L. akamushi* and *L. deliense*, and two sections of the mt genome of *L. fletcheri*. The mt genomes of *L. akamushi* and *L. deliense* are circular and have 13,698 and 13,731 bp, respectively. Both mt genomes have the 37 genes that are typical of Metazoa, but both genomes have two *LNR*s rather than one *LNR*, which is typical of Metazoa. These two mt genomes are substantially smaller (by 3081 and 3048 bp, respectively) than that of *L. pallidum* (16,779 bp) because *L. pallidum* has an extra gene for large-subunit rRNA (*rrnL#2*), a pseudo-gene for small-subunit rRNA (*PrrnS*), and two extra *LNR*s (nos. 3 and 4), compared to *L. akamushi* and *L. deliense* (Fig. 1).

The arrangement of genes and *LNR*s in the mt genome of *L. akamushi* is identical to that of *L. deliense*. *L. fletcheri* apparently also has this arrangement of genes and *LNR*s, but we sequenced only two sections (4.7 kb long in total) of its mt genome (Fig. 1). The arrangement of mt genes and *LNR*s of *L. akamushi* and *L. deliense* differs substantially from that of the hypothetical ancestor of the arthropods inferred by Staton et al. (1997), since (1) 30 of the 39 gene boundaries in the mt genomes of *L. akamushi* and *L. deliense* are novel for an arthropod, (2) at least 16 of their 37 genes have changed position, and (3) another 10 genes have changed both position and orientation of transcription relative to their counterparts of the ancestor of the arthropods (Fig. 1). The arrangement of genes and *LNR*s of *L. akamushi*, *L. deliense*, and *L. fltecher* also differs from that of *L. pallidum* in that (1) five novel gene boundaries, which are associated with the extra *rrnL*, *PrrnS*, and two extra *LNR*s, in the mt genome of *L. pallidum* are not present in *L. akamushi*, *L. deliense*, and *L. fletcheri*; and (2) *trnQ* is between *rrnS* and an *LNR* in *L. pallidum* but is between *trnY* and *rrnL* in *L. akamushi*, *L. deliense*, and *L. fletcheri* (Fig. 1).

Reduced Sizes of Mitochondrial Genes of Leptotrombidium *Species*

The mt genes of *L. akamushi*, *L. deliense*, and *L. fletcheri* have the same or similar sizes as their counterparts in *L. pallidum* (Table 2). The mt genes of these four *Leptotrombidium* species are shorter or substantially shorter (by 0.4–30.1%; Table 2) than their counterparts in *D. yakuba*, which are in the middle range among those of the arthropods studied (Crease 1999; Navajas et al. 2002). Like those of *L. pallidum*, the inferred mt proteins of *L. akamushi*, *L. deliense*, and *L. fletcheri* also lack part of the domains that are present in *D. yakuba* (data not shown but see Shao et al. 2005a). Most of the inferred mt tRNAs of *L. akamushi*, *L. deliense*, and *L. fletcheri* lack stem-and-loops on either the D-arm or the T-arm and, thus, cannot form the conventional cloverleaf structures (Fig. 2). The fact that the unusual secondary structures of tRNAs we found in *L. pallidum* are also conserved in *L. akamushi*, *L. deliense*, and *L. fletcheri* provides additional evidence to our view that the mt tRNA genes of *L. pallidum* encode a complete set of the functional tRNAs, in spite of their unusual secondary structures (Shao et al. 2005a).

We misannotated the size of *rrnL* of *L. pallidum* as 1282 bp in Shao et al. (2005a). In that paper, we could not determine accurately the 5′-end of *rrnL* of *L. pallidum* because an *LNR* lies upstream *rrnL*. In *L. akamushi*, *L. deliense*, and *L. fletcheri*, however, *trnQ* lies upstream of *rrnL*; this allows us to determine the 5′-end of *rrnL* with more accuracy than in *L. pallidum*. We annotated the 5′-end of *rrnL* of *L. akamushi*, *L. deliense*, and *L. fletcheri* as the first nucleotide downstream of *trnQ*. By alignment and comparison of nucleotide sequences, we annotated that *rrnL* of *L. pallidum* is 1008 bp long, which is similar to that of *L. akamushi* (1014 bp), *L. deliense* (1024 bp), and *L. fletcheri* (1014 bp; Table 2). The 274 bp that we misannotated as part of *rrnL* of *L. pallidum* in Shao et al. (2005a) has no significant similarity to any mt genes; we thus annotated this 274

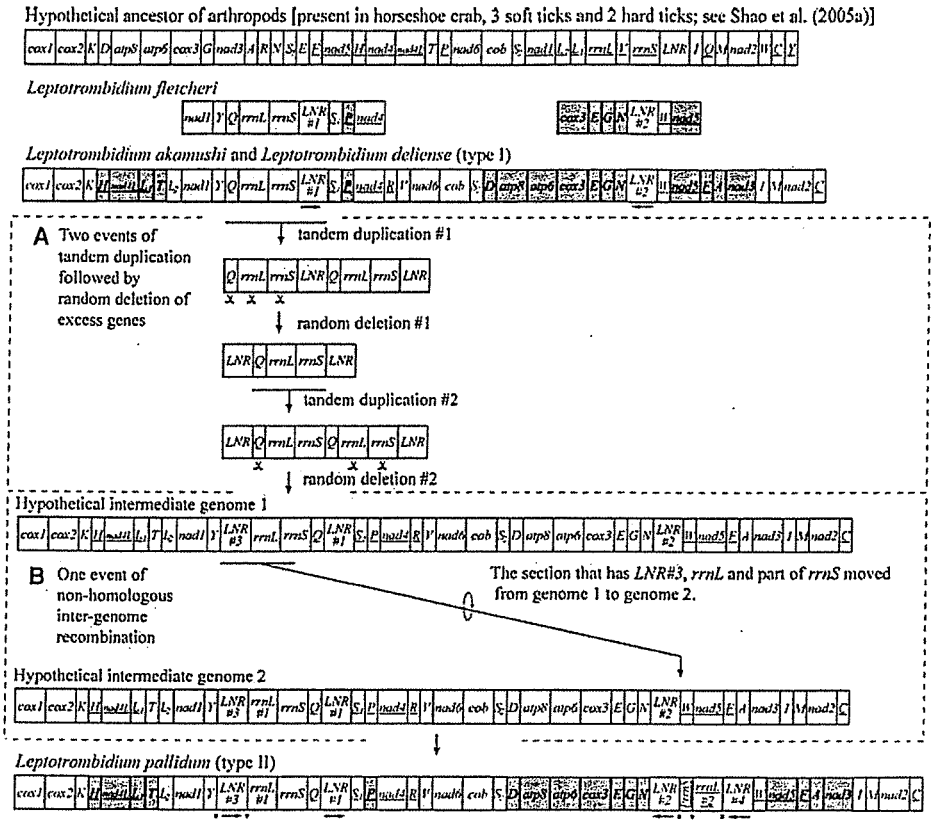

Fig. 1. The mitochondrial (mt) genomes of the hypothetical ancestor of the arthropods and the four *Leptotrombidium* species. The circular mt genomes were linearized at the 5′-end of *cox1* to aid comparison of their gene content and gene arrangement. Two events of tandem duplication followed by random deletion of excess genes (A), followed by one event of nonhomologous intergenome recombination (B), is the simplest scenario for the evolution of the type of mt genome present in *L. pallidum* from the type present in *L. akamushi*, *L. deliense*, and *L. fletcheri*. Dark-gray boxes represent genes that changed positions relative to the ancestor of the arthropods; light-gray boxes represent genes that changed both position and orientation of transcription. The arrow line below an *LNR* indicates the orientation of transcription of that *LNR* relative to that of other *LNR*(s). Scissor symbols represent deletions of excess genes. The circling arrow indicates a change in the orientation of transcription from left-to-right to right-to-left. Asterisks indicate gene boundaries that are present in *L. pallidum* but not in the other three *Leptotrombidium* species. Note that *LNR#3* of the hypothetical intermediate genome 1 became *LNR#4* of *L. pallidum* after nonhomologous intergenome recombination (B). Protein-coding and rRNA genes are abbreviated *atp6* and *atp8* (for ATP synthase subunits 6 and 8), *cox1-3* (for cytochrome *c* oxidase subunits 1–3), *cob* (for cytochrome *b*), *nad1-6* and *4L* (for NADH dehydrogenase subunits 1–6 and 4L), and *rrnL* and *rrnS* (for large- and small-subunit rRNAs). tRNA genes are shown with the single-letter abbreviations of their corresponding amino acids. The two tRNA genes for leucine are L_1 (anticodon nag) and L_2 (yaa), and those for serine are S_1 (nct) and S_2 (nga). Genes are transcribed from left to right except those that are underlined, which are transcribed from right to left.

bp as part of the *LNR* that lies upstream of *rrnL* (see also the section below).

The average length of *rrnL* of the four *Leptotrombidium* species we studied is shorter by 23.5% than its counterpart in *D. yakuba* (Table 2). This is also the case for *rrnS* in these four *Leptotrombidium* species—its average length is shorter by 23.4% than its counterpart in *D. yakuba*. We constructed the secondary structures of the large- and small-subunit (LSU and SSU) rRNAs of *L. pallidum* to identify which domains of LSU and SSU rRNAs were absent due to the substantial size -reduction of *rrnL* and *rrnS*. In comparison with that of *D. yakuba*, the LSU rRNA of *L. pallidum* lacks all the helixes and nucleotides from helix D2 to the 5′-end, including D1, C1, B20, B12, B11, and B9′ (Fig. 3A). All the helixes from D2 to the 3′-end in the LSU rRNA of *D. yakuba* are present in *L. pallidum*, except G13. The SSU rRNA of *L. pallidum* also lacks the helixes at the 5′-end that are present in *D. yakuba*, including helixes 12, 8, 7, 6, 5, 4, 2, and 1 (Fig. 3B). In the middle of SSU rRNA, helix 22 is absent in *L. pallidum*. Only one helix each is present in *L. pallidum* in the section where three helixes, 24, 25, and 26, are present, and in the section where four helixes, 39, 40, 41, and 42, are present in *D. yakuba*. We did not construct secondary structures for the LSU and SSU rRNAs of *L. akamushi*, *L. deliense*, and *L. fletcheri*. However, the domains of LSU and SSU rRNAs that are absent in *L. pallidum* are likely to be absent in these three species too, because *rrnL* and *rrnS* of these three species have the same or similar sizes to those in *L. pallidum* (Table 2) and share a high nucleotide sequence similarity with those in *L. pallidum* (data not shown).

Table 2. Comparison of the sizes of mitochondrial genomes and genes of the chigger mite *Leptotrombidium* species with those of the fruit fly *Drosophila yakuba*

Genome/ Gene	*La*[a]	*Ld*	*Lp*	*Dy*	%[b]	Gene	*La*	*Ld*	*Lf*	*Lp*	*Dy*	%	Gene	*La*	*Ld*	*Lf*	*Lp*	*Dy*	%
Genome	13,698	13,731	16,779	16,019		*rrnS*	608	601	608	601	789	23.4	*trnN*	50	48	49	50	65	24.2
atp6	624	624	621	672	7.3	*rrnL*	1,014	1,024	1,014	1,008	1,326	23.5	*trnP*	56	54	56	52	64	14.8
atp8	147	147	147	159	7.5	*trnA*	49	47		47	65	26.7	*trnQ*	53	53	53	53	69	23.2
cox1	1,530	1,530	1,530	1,536	0.4	*trnC*	55	53		52	63	15.3	*trnR*	48	50		56	64	19.8
cox2	648	648	648	684	5.3	*trnD*	62	62		58	68	10.8	$trnS_1$	50	53	51	54	68	23.5
cox3	777	777	777	786	1.1	*trnE*	60	63	63	59	68	9.9	$trnS_2$	53	51		52	66	21.2
Cob	1,056	1,056	1,056	1,134	6.9	*trnF*	55	56		54	66	16.7	*trnT*	59	57		55	65	12.3
Nad1	879	873	879	972	9.8	*trnG*	53	49	49	50	65	22.7	*trnV*	51	50		50	72	30.1
Nad2	882	882	882	1023	13.8	*trnH*	52	56		54	66	18.2	*trnW*	56	58	56	56	67	15.7
Nad3	303	303	303	351	13.7	*trnI*	49	48		50	65	24.6	*trnY*	48	48	51	49	68	27.9
Nad4	1,230	1,230	1,224	1,338	8.2	*trnK*	60	55		57	71	19.2	*LNR#1*[c]	262	291	365	483	1,077	
Nad4L	255	255	255	288	11.5	$trnL_1$	56	56		54	65	14.9	*LNR#2*	259	300	366	509		
Nad5	1,536	1,536	1,536	1,719	10.6	$trnL_2$	64	66		60	66	4.0	*LNR#3*				734		
Nad6	426	426	426	522	18.4	*trnM*	65	63		61	69	8.7	*LNR#4*				746		

[a] *La, L. akamushi; Ld, L. deliense; Lf, L. fletcheri; Lp, L. pallidum; Dy, D. yakuba.*
[b] $\% = [Dy - (La + Ld + Lp)/3]/Dy \times 100$ or $\% = [Dy - (La + Ld + Lf + Lp)/4]/Dy \times 100$ if the length of a gene of *L. fletcheri* is known.
[c] The number of *LNR*s does not indicate the homology of these *LNR*s.

Duplicate and Quadruple Large Noncoding Regions of Leptotrombidium *Species*

Both *L. akamushi* and *L. deliense* have two *LNR*s in their mt genomes. The two *LNR*s of each of these two species have similar sizes and near-identical nucleotide sequences (Tables 2 and 3) but have opposite orientations of transcription (Fig. 1). *L. fletcheri* also has two near-identical *LNR*s, which are in the same relative positions as the two *LNR*s of *L. akamushi* and *L. deliense*. Relative to *L. akamushi*, *L. deliense*, and *L. fletcheri*, *L. pallidum* has two extra *LNR*s (nos. 3 and 4; see Fig. 1). The four *LNR*s of *L. pallidum* have sections with near-identical nucleotide sequences (Table 3), but these four *LNR*s differ substantially in size and have opposite orientations of transcription (Table 2, Fig. 1). The two or four *LNR*s of a *Leptotrombidium* species are more similar to each other in size and nucleotide sequence than they are to the *LNR*s of other *Leptotrombidium* species (Table 3). In a similar vein, our phylogenetic analysis of the *LNR* sequences revealed that the two or four *LNR*s of each *Leptotrombidium* species are more closely related to each other than they are to the *LNR*s of other *Leptotrombidium* species (Fig. 4).

Discussion

Evolution of Two Types of Mitochondrial Genome in the Genus Leptotrombidium

Our results reported above revealed two types of mt genome in the genus *Leptotrombidium*: one is present in *L. akamushi*, *L. deliense*, and, apparently also, *L. fletcheri*; the other is present in *L. pallidum*. These two types of genome differ in genome size, gene content, and arrangement of *trnQ* but share reduced sizes of genes and the arrangement of all genes other than *trnQ*. It is unusual that species of the same genus differ in gene content and gene arrangement in their mt genomes, since gene content and gene arrangement are generally conserved at low taxonomic levels (see Boore 1999). The results above prompted us to ask two questions. First, between the two types of mt genome, which one is more likely to be ancestral to *Leptotrombidium*, and which one is more likely to be derived to *Leptotrombidium*? Second, what mechanisms of gene rearrangement were likely involved in the evolution of the mt genomes of the *Leptotrombidium* species from one type to another?

In order to address the first question, an outgroup is needed with which the *Leptotrombidium* species can be compared. In the absence of data from any outgroup species that are closely related to *Leptotrombidium*, we chose the hypothetical ancestor of the arthropods as an outgroup for the comparison of mt gene content and gene arrangement with *Leptotrombidium* species. The ancestor of the arthropods is a meaningful outgroup for such comparison, in our view, because both types of mt genome of the *Leptotrombidium* species can be viewed as being derived from the ancestral type of mt genome of the arthropods. Further, the gene content and gene arrangement of the ancestral type of mt genome of the arthropods remain unchanged in at least five species of the Acari studied (Shao et al. 2005a), suggesting that the ancestor of the Acari and some lineages of the Acari have the same mt gene content and gene arrangement as the ancestor of the arthropods. By comparison of the gene content and gene arrangement of the two types of mt genome of the *Lepto-*

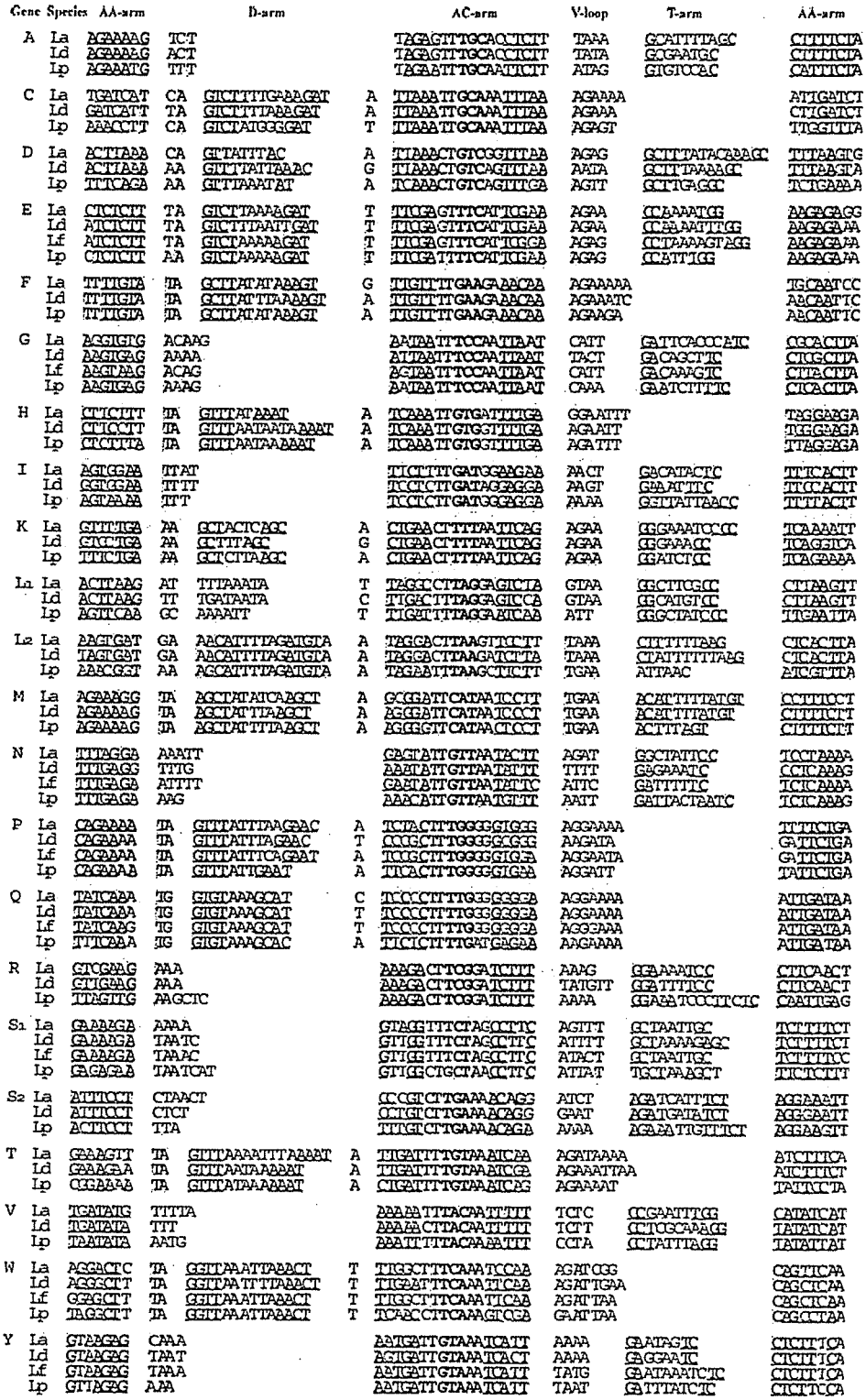

Fig. 2. Alignment of the sequences of the mitochondrial tRNA genes of *Leptotrombidium akamushi* (La), *L. deliense* (Ld), *L. fletcheri* (Lf), and *L. pallidum* (Lp). tRNA genes are named with the single-letter abbreviations of their corresponding amino acids. Nucleotides that pair at the arms are underlined. Sequences of anticodons are in boldface. Conserved nucleotides are shaded in gray.

trombidium species with those of the ancestral type of mt genome of the arthropods, we propose that it is more parsimonious to infer that the type of mt genome present in *L. pallidum* (with 37 genes typical of Metazoa, four *LNRs*, an extra *rrnL*, and a *PrrnS*; hereafter type II) evolved from the type of mt genome

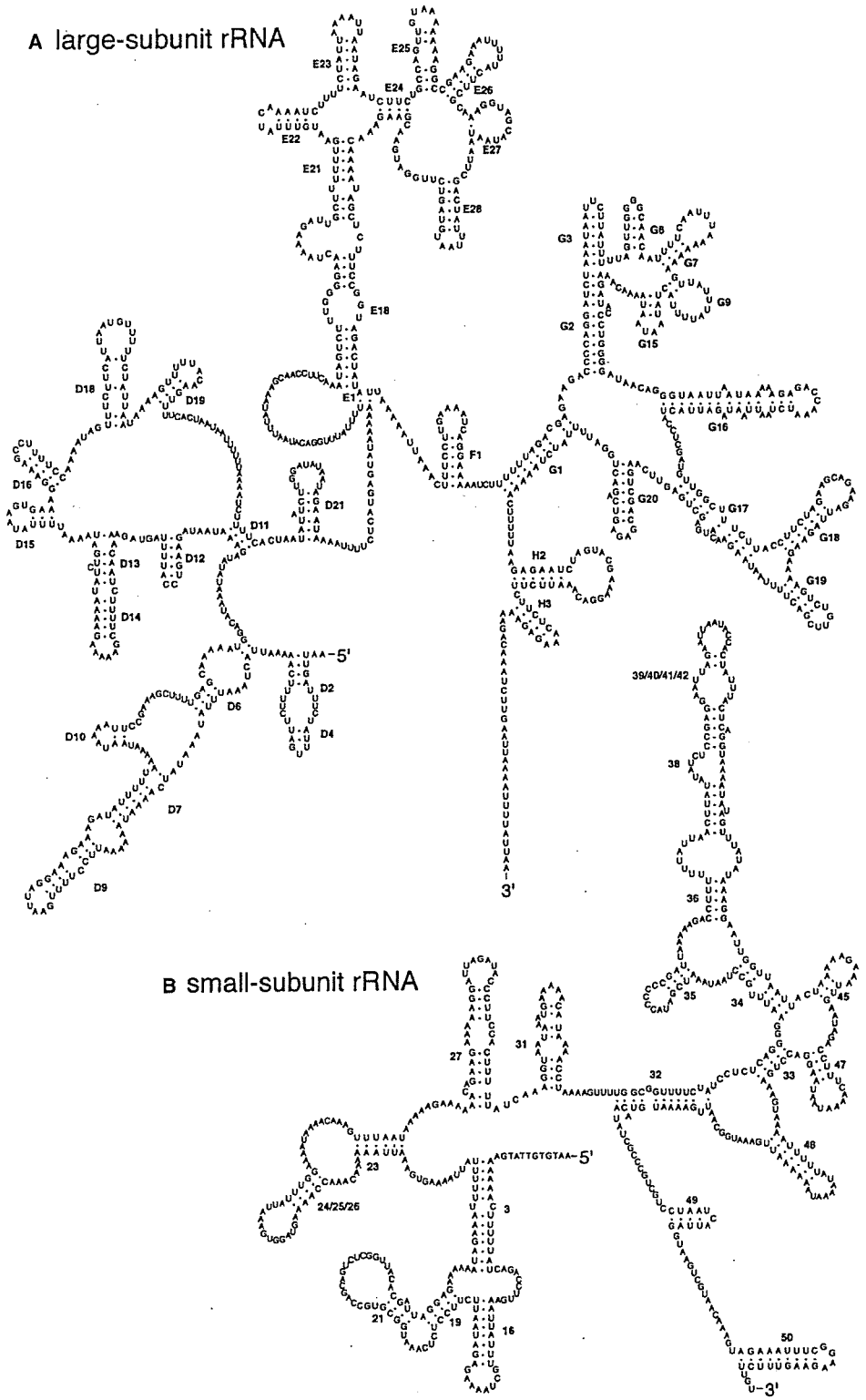

Fig. 3. Putative secondary structures of the large-subunit rRNA (A) and the small-subunit rRNA (B) of *Leptotrombidium pallidum*. Dots indicate Watson-Crick bonds and bonds between U and G. The numbering of the helixes is after de Rijk et al. (1997) for large-subunit rRNA and after van de Peer et al. (1997) for small-subunit rRNA.

present in *L. akamushi*, *L. deliense*, and *L. fletcheri* (with 37 genes and two *LNR*s; hereafter type I) (Fig. 5A) than vice versa (Fig. 5B). There are three lines of evidence for our proposal. First, it requires *three events of duplication* to account for the evolution of two *LNR*s in the type I genome from one *LNR*